Clin Oral Invest (2013) 17:1709–1717
DOI 10.1007/s00784-012-0870-6

ORIGINAL ARTICLE

Proteomic and scanning electron microscopic analysis of submandibular sialoliths

József Szalma · Katalin Böddi · Edina Lempel · Alexandra Forsayeth Sieroslawska · Zoltán Szabó · Rania Harfouche · Lajos Olasz · Anikó Takátsy · András Guttman

Received: 11 June 2012 / Accepted: 17 October 2012 / Published online: 27 October 2012

Abstract
Objectives Several theories have been proposed regarding the genesis of sialoliths, including the organic core theory, which suggests epithelial or bacterial etiology originating in the central core. Our aim was to use novel methodologies to analyze central areas (the core) of calculi from sialolithiasis patients.
Materials and methods The structures of the halves of six submandibular salivary stones were analyzed by scanning electron microscopy (SEM). After structural analysis, from the other six halves, samples from the central parts of the core and peripheral parts of the core were digested with trypsin and analyzed by matrix-assisted laser desorption ionization–time of flight mass spectrometry. The peptide mass fingerprints were compared with the results of in silico digestion.
Results SEM analysis of the sialoliths showed that organic structures (collagen/fibrous-like structures, bacterial fragments) were visible only outside of the core in the concentric layers of external areas, but not in the core area. The mass spectrometry (MS)/MS post-source decay experiments were completed from the four, most intense signals observed in the MS spectrum and human defensin was proven to be present in three of the examined samples, originated from the peripheral region of three cores.
Conclusions Although proteomic analysis demonstrated defensin protein in the peripheral region of the core in three sialoliths, SEM failed to prove organic structures in the core.
Clinical relevance New investigation modalities still cannot prove organic structures in the core, henceforward challenging the organic core theory.

Keywords Sialolith · Calculus · Etiology · Submandibular gland · SEM · MALDI-TOF · Defensin

J. Szalma (✉) · E. Lempel · A. F. Sieroslawska · L. Olasz
Department of Oral and Maxillofacial Surgery, University of Pécs,
5. Dischka Street,
Pécs 7621, Hungary
e-mail: jozsef.szalma@aok.pte.hu

K. Böddi · Z. Szabó · A. Takátsy
Department of Biochemistry and Medical Chemistry,
University of Pécs,
Pécs, 12. Szigeti Street,
Pécs 7624, Hungary

R. Harfouche
Harvard-MIT Division of Health Sciences and Technology,
Harvard Medical School,
65 Landsdowne Street,
Cambridge, MA 02139, USA

A. Guttman
Horváth Laboratory of Bioseparation Sciences,
University of Debrecen,
98. Nagyerdei krt,
Debrecen 4032, Hungary

Introduction

Sialolithiasis is one of the most common causes of obstructive salivary gland diseases, occurring worldwide in 0.1 to 1 % of the population [1, 2]. It is characterized by partial or total salivary stagnation associated with pain, swelling, and possible retrograde infection of affected gland [1, 2]. Obstructions mainly occur in the submandibular gland and the Wharton's duct rather than the parotid gland or the parotid duct since there are two bends in the Wharton's duct and the submandibular saliva travels against gravity. The

higher viscosity submandibular saliva has higher content of mucin and calcium salts [3–7].

Kasaboglu et al. [8] described sialoliths as a composition of organic and inorganic matrices having a central core and a laminar peripheral structure with calcium phosphate as major component. The stones are reportedly composed of 18 % organic and 82 % inorganic material [9]. Another investigation showed that the organic components contain approximately 5–6 % (of stone weight) proteins and 1 % lipids [10]. Inorganic components are mainly calcium phosphates (hydroxyapatite, brushite, whitlockite, and octacalcium phosphate) and carbonates [11–14].

Prevalent theories of stone formation include the (1) organic core theory; calcification of bacteria, foreign body, or desquamated epithelial cells; (2) microlith theory: normally present in 80 % of submandibular glands; and the (3) mucoepidermoid gel theory: calcification on high viscosity mucins [13, 15–17]. Grases et al. [1] concluded that stone formation depended on the presence of some kind of organically retained material (e.g., mucins) and on the balance of a high hydroxyapatite to crystallization inhibitors, like phytate, salivary magnesium, and citric acid.

In 1988, matrix-assisted laser desorption/ionization (MALDI)–mass spectrometry (MS) was introduced by Karas et al. [18]. MALDI-MS is highly sensitive and rapid, not limited to measuring the mass of intact analyte molecules. The sample containing the analyte of interest is mixed and co-crystallized with matrix solution (generally small aromatic organic acids). The matrix is very important, it serves to absorb the laser radiation, prevent the analyte from the direct laser 'hit', and transport the energy to the analytes. The laser beam introduced to the molecules of the matrix, desorbed and ionized the analyte molecules that are produced protonated molecules of the analytes [19]. Time-of-flight mass analyzers are used for accurate mass measurement and peptide sequencing. The ions are separated on the basis of their *m*/*z* values. Complex protein mixtures are enzymatically digested (bottom–up approach) into complex peptide mixture before the mass spectrometric measurement. First the masses of intact peptides are determined (peptide mass fingerprint (PMF)), then these peptide ions are selected and fragmented to gain information on their sequence and modifications (MS/MS). MS/MS spectra are recorded for as many peptides as possible and the results used to search databases to identify the protein in the original mixture [20–22]. One critical problem is that suppression effect between the analyte molecules is still frequently arising. The probability of signal suppression effects increases with higher analyte complexity.

Among mass spectrometric approaches, the bottom–up technique was used in our study to identify the possible protein candidates extracted from sialoliths [23]. After the subsequent enzymatic digestion with trypsin, the resulted peptide pool was analyzed by MALDI-TOF/MS. The latter was chosen because of its sensitivity (down to low femtomole level) [24]. Additional advantages of using MALDI are that during the ionization process, mainly single charged ions are formed that makes the identification/data processing easier. MALDI is also known to tolerate moderate concentration of salts originating from different sources such as digestion buffers [25].

The aim of our study was to combine ultrastructural visualization and proteomic approaches using SEM and MALDI-TOF, respectively, to investigate possible protein structures of sialoliths. The total proteomic analysis of salivary stones or protein-rich periphery was not an aim, but rather the exact analysis of the presumably related core with lithogenesis.

Materials and methods

Study design

Patient selection was limited to cases where salivary calculi were located extra-glandular, in the Wharton's duct. Fifteen submandibular salivary stone removals were processed between July 2007 and August 2008 in the Department of Oral and Maxillofacial Surgery (University of Pécs, Pécs, Hungary). Before the operation, each patient provided fully informed consent. The study was approved by the Regional Research Ethics Committee of the Medical Center, Pécs (no. 4321.316-2671/KK15/2011). Each stone was removed following local anesthesia with block anesthesia of the lingual nerve and with terminal infiltration of the sublingual area (2 % lidocain with 0.001 % adrenalin). Immediately after removal, calculi were collected in sterile Eppendorf tubes containing 4 % neutrally buffered (with phosphates) formaldehyde solution (Molar Chemicals, Budapest, Hungary). Seven stones, below 6 mm in diameter, were excluded from this study due to the limited size of the core and to the difficulties of sample preparation. Thereafter, each calculus was cut into halves, one of which was used for SEM. Two further calculi—without a clearly visible core—were excluded from the study because the examination of the core was not possible (Fig. 1a).

SEM analysis

For SEM observation, the calculi were dehydrated in a graded ethanol series, air dried, and coated with a thin film of evaporated gold. SEM observations were performed by JEOL JSM 6300 microscope (Tokyo, Japan) between ×20 and ×20,000 magnification.

MALDI-TOF analysis

For MALDI-TOF analysis, 1-mm^3 specimens were isolated from the center of the core, as well as from the peripheral areas of the core, as illustrated in Fig. 1b.

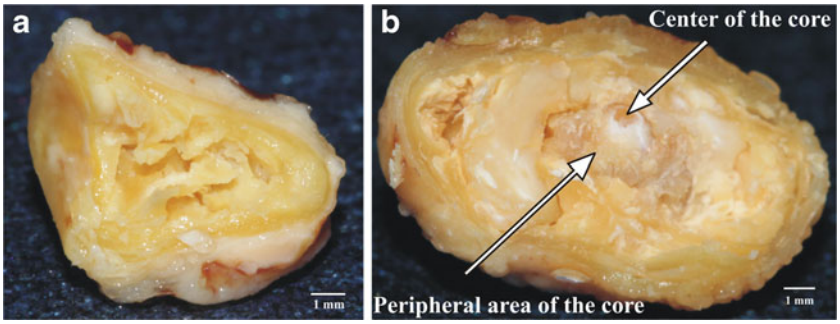

Fig. 1 Photographs of salivary stones. Calculi, without clearly identifiable core—represented in picture (**a**)—were excluded from the study, whereas stones showing a significant core (**b**) were kept for further examination. Samples for MALDI-TOF/MS analysis were taken from the center of the nucleus of the calculi and from the peripheral area of the core as illustrated (**b**)

Chemicals

Acetonitrile, (gradient grade) trifluoroacetic acid (TFA, ≥99 %), α-cyano-4-hydroxycinnamic acid (CHCA, ≥99 %), D/L-dithiothreitol (DTT, >99 %), iodoacetamide (≥98 %), 2-mercaptoethanol (≥98 %), ammonium bicarbonate (>99 %), and urea were purchased from Sigma-Aldrich (Budapest, Hungary). Peptide calibration standard (consisting of bradykinin, angiotensin II, angiotensin I, substance P, renin substrate, ACTH clip (1–17), ACTH clip (18–39), and somatostatin) and was obtained from Bruker Daltonics (Bremen, Germany). Trypsin (sequencing grade, modified) was provided by Promega Corporation (Madison WI, USA). Bidistilled water was prepared in our laboratory.

Tryptic digestion of calculi in solution

The samples were ground, extracted with urea, digested with trypsin, and then analyzed by MALDI-TOF (Autoflex II MALDI instrument, Bruker Daltonics, Bremen, Germany).

The grinded salivary stones were dissolved in 400 μl denaturing buffer consisting of 8 M urea and 0.5 M ammonium bicarbonate (pH7.8), and shaken for 30 min at 37 °C. After the denaturation step, centrifugation was performed for 5 min at 10,000 rpm, in order to sediment the inorganic part. Thereafter, 30 mM (15 uL) DTT solution was added to the supernatant to break the disulfide bonds (37 °C, 30 min). After the solution cooled down, 25 μl of 100 mM iodoacetamide solution was added for 15 min in darkness to alkylate the cysteine groups. The reaction was stopped by the addition of 50 μl 100 mM β-mercaptoethanol and the mixture was kept at ambient temperature for 15 min. The solutions were then filtered through Microcon Ultracel YM-3 membrane with a 3,000-Da cutoff, centrifuged (14,000×*g*, 60 min), and washed with 400 ml distilled water three times. This step ensured the removal of excess substances through the membrane. After the fourth centrifugation, the residues of the modified proteins were recovered at 1,000×*g* (3 min) and digested with 250 ng trypsin in 50 mM ammonium bicarbonate solution overnight at 37 °C. The digestion was ceased by adding 10 μL of 0.01 M TFA solution to the digests. Once the digests were lyophilized, the peptides were redissolved in 5 μL of water and analyzed.

The samples and the matrices solution were co-crystallized on MTP 384 ground steel MALDI target plate.

MALDI-TOF/MS conditions

A solution of 8 mg/ml alpha-cyano-4-hydroxycinnamic-(matrix) in 50 % acetonitrile and 0.1 % trifluoroacetic acid was mixed with 1-μl sample in a 1:1 ratio on the target plate. All mass spectra were monitored in positive mode with pulsed ionization (λ=337 nm; nitrogen laser, maximum pulse rate, 50 Hz, maximal intensity 20–30 % of the laser for peptides). Peptides digests were measured in reflectron mode using delayed extraction of 120 ns. The accelerating voltage was set to +19 kV; the reflectron voltage was set to +20 kV. Spectra of peptides were the sum of 1,500 shots. Prior to each measurement, external calibration was implemented using Pepmix I (Bruker Daltonics). The detection was made in the 800–4,000 *m/z* range. The resulted PMF was analyzed using Mascot data search engine (Matrix Science Inc., Boston, USA).

Data processing was accomplished with Flex Analysis software packages (version 2.4., Bruker Daltonics, Bremen, Germany). For the in silico digestion Sequence Editor Software (Bruker Daltonics, Bremen, Germany) and the database search, the following criteria were chosen: (1) all cysteines were treated with iodoacetamide; (2) monoisotopic masses were allowed; and (3) the maximum number of missed cleavage sites was two.

For the database search, the subsequent settings were applied—database: NCBI or SwissProt; entries: all entries or human; fix modification: carbamidomethyl (C); possible modification: oxidation on methionine; enzyme: trypsin; number of missed cleavage, two; peptide mass tolerance, 100 ppm; and fragment mass tolerance, 50 ppm.

In every single case, searching in NCBI or SwissProt database and the applied search with all entries or human the defensin was the significant result in all the three samples.

Results

Scanning electron microscopy

Sialoliths presented highly mineralized smooth and very dense core surrounded by amorphous-looking (honeycomb-like) structures (Fig. 2a). This core structure was surrounded by columnal or pyramidal structures (Fig. 2b) or at more peripherally by lamellar structures (Fig. 2c). The external surface was coarse, in most of the cases, and usually presented with a globular or nodular appearance, although in a few cases the external surface was smooth (Fig. 2d). The SEM analysis failed to prove any organic structures in the core of calculi, whereas peripheral concentric lamellar structures consisted of different types of fine fibrous-like or microorganism-like inclusions (Fig. 2e–f).

MALDI-TOF analysis

Peptide mass fingerprint measured from the tryptic digestion of the extracted protein (Fig. 3) was analyzed by data search engine under the abovementioned criteria. The identified protein was the A chain of defensin HNP-3, with a nominal mass of 3,832. The score value of the hit was high (79) which serves as an evidence for the reliability of the identification. The sequence of this chain was *DCYCR**IPACI AGERRYGTCI YQGR**LWAFCL* and was given with a one-letter code. The identified part of this sequence is written in bold.

To be able to gain information about the sequence coverage measured, defensin HNP-3 was digested virtually (in silico digestion). PMFs were compared to the in silico

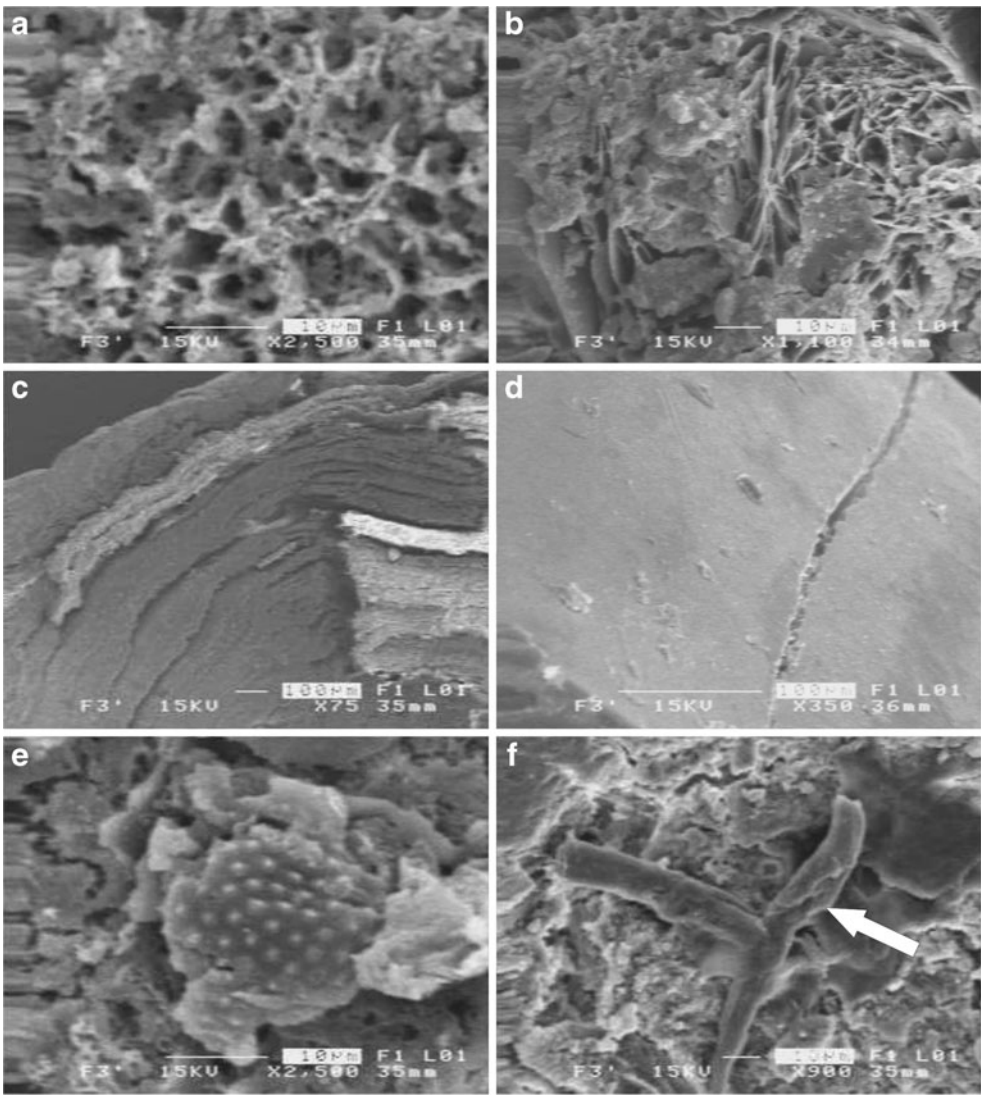

Fig. 2 Scanning electron micrographs from submandibular salivary stones. **a** Honeycomb-like structure of the central area of the core; **b** columnal and irregular structures of the perypheral parts of the core; **c** concentric, lamellar structure of the peripheral parts of the calculus; **d** unusual smooth appearance of the external surface of the calculus; **e** microorganism-like structure (probably bacteria) in the periphery; **f** collagen-like fibrous structure (*arrow*) on the broken surface in the peripheral area adjacent to the core

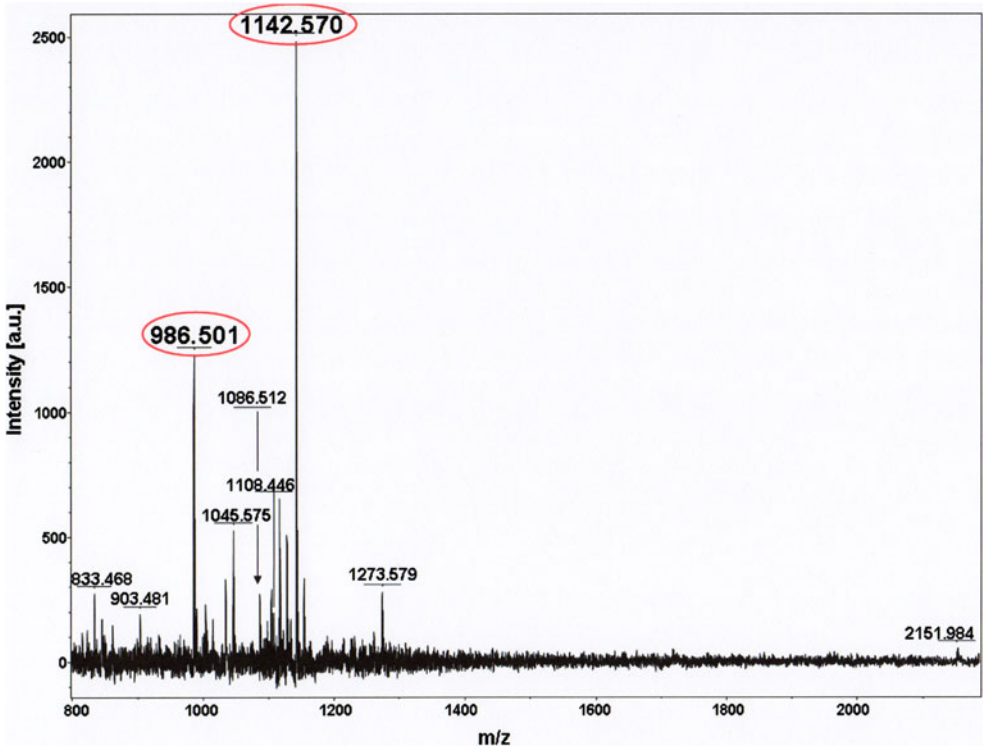

Fig. 3 Peptide mass fingerprint of the sample extracted from salivary calculus no. 3 from peripheral area of the core

(virtually digested) peptides to gain information about the sequence of the protein of interest. Peptides that resulted from this software-assisted, virtual digestion are shown by Table 1. Theoretical masses, experimental masses of the peptides, and the delta masses (in parts per million) can also be seen in Table 1.

As a matter of fact, from the result of the in silico digestion four peptides with *m/z* 986.501, 1,142.570, 1,273.579, and 1,117.501 (Table 1) were found to be identical with those measured from the PMF (Fig. 3). The start and end position (in the amino acid sequence of the protein) of these peptides are 6–14, 6–15, 15–24, and 16–24 and the corresponding mass error values were low (average errors were −73.43, 11.7, and 19.44 ppm, with mass tolerance range of 100 ppm). The sequence coverage of the identified protein was found to be 63 % which is shown by Fig. 4. Out of the 30 amino acids of A chain of defensin HNP-3, mass spectrometric measurements allowed to identified 19 amino acids, as shown by Fig. 4.

To further support our results, the first two peptides (with masses of 986.496 and 1,142.585) were chosen as parent

Table 1 In silico digestion of the defensin

Range	Partials	Sequence	Theoretical mass	1		2		3	
				Experimental mass	Delta mass (ppm)	Experimental mass	Delta mass (ppm)	Experimental mass	Delta mass (ppm)
[1–5]	0	DCYCR	773.27						
[1–14]	1	DCYCRIPACIAGER	1,740.761						
[1–15]	2	DCYCRIPACIAGERR	1,896.862						
[6–14]	0	IPACIAGER	986.509	986.429	−80.7	986.52	11	986.501	−7.65
[6–15]	1	IPACIAGERR	1,142.61	1,142.51	−83.9	1,142.61	−4.63	1,142.57	−37.4
[6–24]	2	IPACIAGERRYGTCIYQGR	2,241.101						
[15–24]	1	RYGTCIYQGR	1,273.61			1,273.58	22.1	1,273.58	−25.1
[15–30]	2	RYGTCIYQGRLWAFCC	2,110.941						
[16–24]	0	YGTCIYQGR	1,117.509	1,117.45	−55.7	1,117.5	−8.58	1,117.5	−7.62
[16–30]	1	YGTCIYQGRLWAFCC	1,954.839						
[25–30]	0	LWAFCC	856.348						

Fig. 4 The sequence coverage of the four identified overlapping peptides

ions in a post-source decay experiments. The fragmentation pattern of these two peptides provides additional evidences concerning the sequence of the protein (Figs. 5 and 6).

Based on the differences between the masses of the amino acid residues (the resulted fragment ions), the sequence of the peptides were determined (IPACIAGER for 986.496 and IPACIAGERR for 1,142.585). MS/MS sequencing gave the same result as the mass search from the Mascot Database, therefore confirmed our results.

Discussion

The exact etiology of calculus formation during sialolithiasis has been the subject of much debate for the past 40–50 years. The prevailing theory, namely the "organic core theory", describes salivary calculus as the apposition of inorganic crystals around an organic matrix [1, 17]. However, a mechanistic proof of the genesis of this disease remains unknown. Degenerative material synthesis into the ductal system seems to have an important role in calculus formation [6]. Salivary stagnation and inflammation and a decrease in pH which decreases solubility of calcium phosphates should promote stone formation, whereas bacterial organisms, epithelial cells, or foreign bodies may be the originating cause of sialolithiasis by causing organelle degeneration [11, 13, 26]. Boskey et al. [10] proposed that initial hydroxyapatite deposition originates on lipids of degenerating cells. Accordingly, Tanaka et al. [13] used ultrastructural analyses to demonstrate that calcifications are observed around degenerative organelles, like lipid-like structures (droplets), mitochondria, and lysosomes. Lee and Wong [26] observed that in minor salivary glands ducts, there are more multiple sialoliths, thus concluding that the ductal epithelium may constitute the nidus of stone formation. Whereas earlier reports (1980s) concluded according to SEM or histologic or microradiographic investigations that "the presence of microorganisms also in the nucleus of the calculus seems to be one important etiological factor favoring the formation of calculi" or "it is possible the glycoproteins of the submandibular gland to act as nucleating sites in the formation of calculi" [27, 28], later investigations mainly after year 1995 (SEM, transmission EM, or X-ray photoelectron spectroscopic studies) have clearly shown that stone formation is not possible via a luminal organic nidus in the absence of identifiable organic organelles in the core [8, 29]. Furthermore—except for the abovementioned investigation [27]—microorganisms have not been described in the core of sialoliths [8], but only in the peripheral parts or the outer shell [17]. According to Hiraide and Nomura's theory [12], foreign body or microorganisms (whose genus

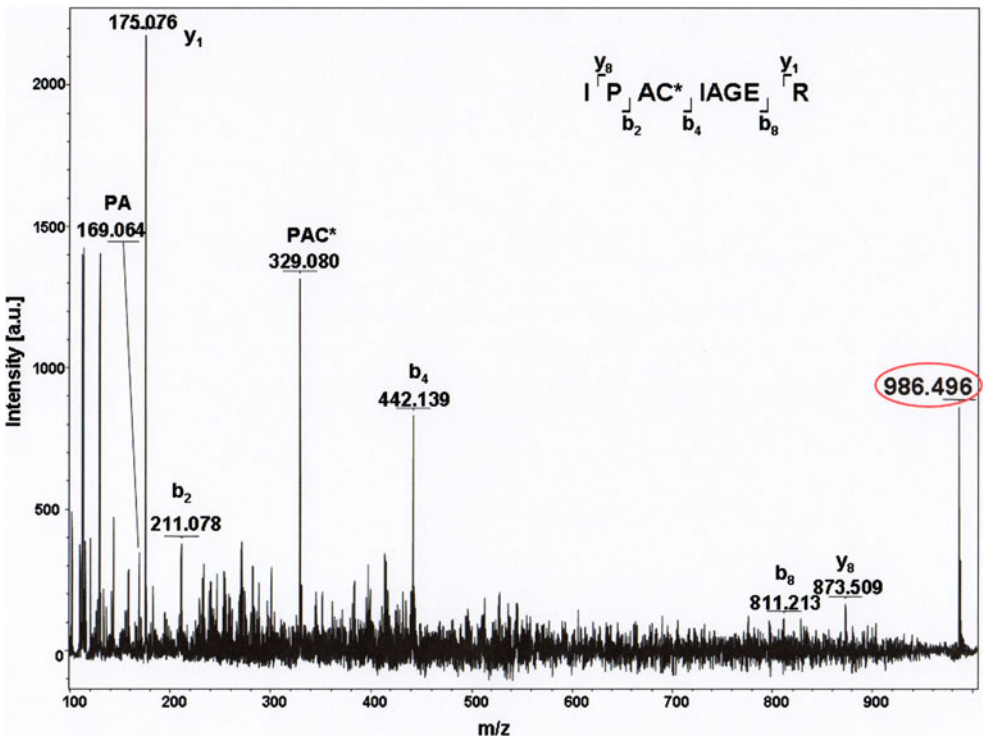

Fig. 5 MS/MS spectrum of the peptide with a mass of 986.496

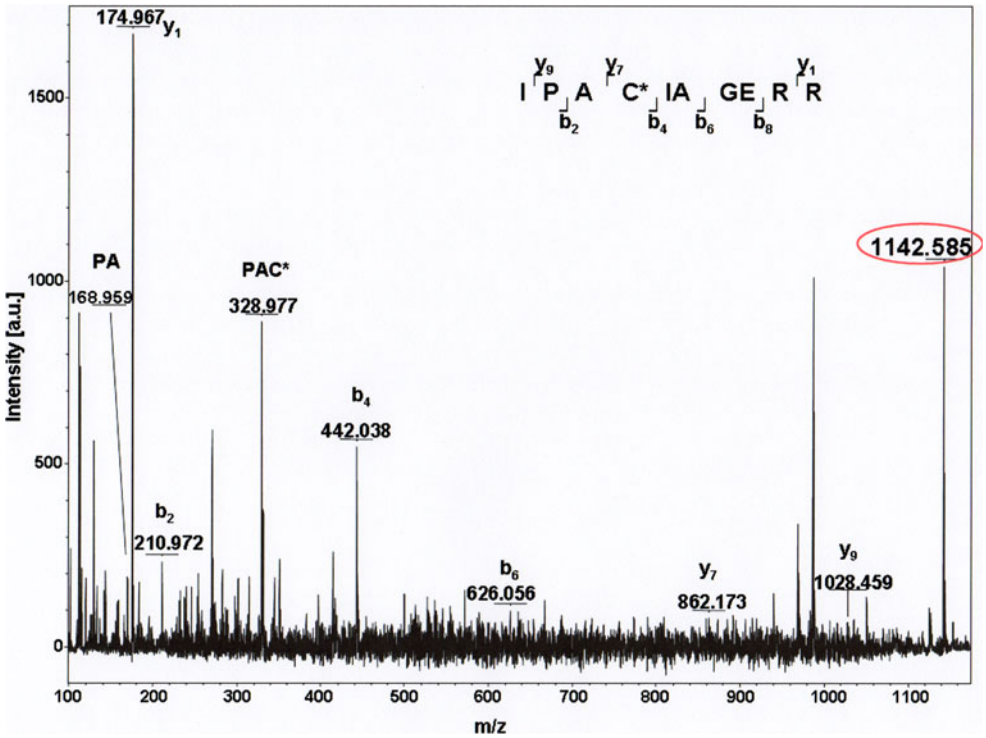

Fig. 6 MS/MS spectrum of the peptide with a mass of 1,142.585

remains unknown) can act as a trigger of initial stone formation, as the nucleus might be morphologically changed during the latter development of stone formation. In contrast, many investigators suggest that stone formation is secondary to sialoadenitis [8, 29, 30]. The swelling during chronic sialoadenitis results in salivary stasis and the calcium-rich secretory material that subsequently forms a calcified core, indicating latter stone formation [30]. In addition, Teymoortash et al. (2002) stated as evident conclusion that the nidus of salivary stones is primarily inorganic [17].

Our ultrastructural investigations proved that organic structures are present in calculi (epithelial cell, fine fibrous-like structure, bacterial fragments) (Fig. 2). It is important to note that similar to previous reports, organelles were not identifiable in the core area [8, 26]. Furthermore, we found that calculi have an amorphous and honeycomb-like appearance devoid of organic structures [8, 11, 13, 17, 29]. In contrary to a previous report that found a nucleus in each sample, we excluded two stones from this study because nidus was not observed [31]. Interestingly, these stones were extracted from multiple calculi cases and both stones were found proximally to the gland, behind significantly sized calculi causing totally obstruction and salivary stagnation in the Wharton's duct.

Earlier reports failed to identify exact protein structures or fragments or their origin in the core of calculi yet, whereas the existence of tryptophan, tyrosine, disulfides, phenylalanine, and hydroxyl proline was suggested in calculus when "total stone" analysis was performed [32, 33]. Teymoortash et al. [17] identified moreover the presence of *Streptococci* and *Peptostreptococci* inclusions in calculi, although they stated clearly that these microorganisms concentrate in the outer layers of the periphery. Whereas total salivary stone protein analysis results show more protein findings (more than ten different identified proteins were present in our researches), these proteins are extracted from outer concentric layers, so according to our opinion, this information correlates rather with appositional growth of calculi, then with initiation. In addition, bigger stones usually result in more proteins [34], but the present study failed to prove more proteins with MALDI from the cores of "giant" calculi (>15 mm). Although, parotid stones usually contain more protein [35, 36], meaning a good alternative for protein analysis, these stones are very rare in our practice (160 submandibular calculi in contrast with just three parotid stones in the last 5 years in our department) and usually are smaller in size than 5 mm as a limitation for core preparation. Moreover, obstructions in the parotid duct are mainly associated with "noncalcified stones or mucous plugs" indicating more difficult selection for analysis [37, 38].

Considering Hiraide and Nomura's core "transformation" theory during stone development, MALDI-TOF was used to elucidate "ultra-structurally invisible" protein structures of the core of calculi. No identifiable protein structures were found in the central areas of the cores, but we reported here the presence of human defensin (also known as HP3, DEF3, HNP3, HP-3, or HNP-3) in the peripheral area of the core of three calculi. Human defensin is a cysteine-rich, cationic,

low molecular mass, antimicrobial peptide produced by a number of epithelial cells, exhibiting potent antimicrobial activity against Gram-negative and Gram-positive bacteria and against fungi [39–42]. Defensin has clear roles in mediating the immune response, and the appearance of this protein in calculi helps to understand the presence of chronic inflammation (sialoadenitis) during the appositional growth of calculi. It would be of interest to investigate the concentrations of different inflammatory proteins (e.g., with antimicrobial activity) in the saliva samples of sialolithiasis patients and the correlation with possible nucleating protein findings in concurrent calculi.

Our MALDI results confirmed our structural observation from SEM, namely that protein structure is identifiable in salivary stones, however never in the central area of the core. Although defensin was present in a calculus near to the nidus, further studies will be required to establish its possible role in sialolithiasis. Our novel approach to combine MALDI-TOF with SEM may open up exciting possibilities to identify novel mechanisms to target during sialolithiasis.

Acknowledgments We would like to thank Professor László Seress for SEM analysis and Béla Dolgos for the SEM technical assistance. The authors thank the Hungarian Scientific Research Fund (OTKA) PD 76395, PD 78599, and K 81839 for supporting this research.

Conflict of interest The authors declare that they have no conflict of interests.

References

1. Grases F, Santiago C, Simonet BM, Costa-Bauza A (2003) Sialolithiasis: mechanism of calculi formation and etiologic factors. Clin Chim Acta 334:131–136
2. Sherman JA, McGurk M (2000) Lack of correlation between water hardness and salivary calculi in England. Br J Oral Maxillofac Surg 38(1):50–53
3. Schow SR, Miloro M (1998) In: Peterson LJ (ed.) Oral and Maxillofacial Surgery. 3rd ed. Mosby, St. Louis, 486–509.
4. Lipa B, Beer-Sheva (2002) Giant salivary gland calculi: diagnostic imaging and surgical management. Oral Surg Oral Med Oral Pathol Oral Radiol Endod 94:320–323
5. Baurmash HD (2007) Obstructive parotid ductal disease: intraoral management. J Oral Maxillofac Surg 65:1886–1891
6. Baurmash HD (2004) Submandibular salivary stones: current management modalitis. J Oral Maxillofac Surg 62:369–378
7. Szalma J, Olasz L, Tóth M, Acs P, Szabó G (2007) Diagnostic value of radiographic and ultrasonic examinations in patients with sialoadenitis and sialolithiasis. Fogorv Szle 100:53–58
8. Kasaboglu O, Er N, Tümer C, Akkocaoglu M (2004) Micromorphology of sialoliths in submandibular salivary gland: a scanning electron microscope and X-ray diffraction analysis. J Oral Maxillofac Surg 62:1253–1258
9. Zenk J, Benzel W, Iro H (1994) New modalities in the management of human sialolithiasis. Minim Invasive Ther 3:275–284
10. Boskey AL, Boyan-Salyers BD, Burstein LS, Mandel ID (1981) Lipids associated with mineralization of human submandibular gland sialoliths. Arch Oral Biol 26:779–785
11. Mimura M, Tanaka N, Ichinose S, Kimijima Y, Amagasa T (2005) Possible etiology of calculi formation in salivary glands: biophysical analysis of calculus. Med Mol Morphol 38:189–195
12. Hiraide F, Nomura Y (1980) The fine surface structure and composition of salivary calculi. Laryngoscope 90:152–158
13. Tanaka N, Ichinose S, Adachi Y, Mimura M, Kimijima Y (2003) Ultrastructural analysis of salivary calculus in combination with X-ray microanalysis. Med Electron Microsc 36:120–126
14. Burnstein LS, Boskey AL, Tannenbaum PJ, Posner AS, Mandel ID (1979) The crystal chemistry of submandibular and parotid salivary gland stones. J Oral Pathol 8:284–291
15. Williams MF (1999) Sialolithiasis. Otolaryngol Clin N Am 32:819–834
16. Anneroth G, Eneroth CM, Isacsson G (1975) Morphology of salivary calculi. The distribution of the inorganic component. J Oral Pathol 4:257–265
17. Teymoortash A, Wollstein AC, Lippert BM, Peldszus R, Werner JA (2002) Bacteria and pathogenesis of human salivary calculus. Acta Otolaryngol 122:210–214
18. Karas M, Hillenkamp F (1988) Laser desorption ionization of proteins with molecular masses exceeding 10,000 daltons. Anal Chem 60:2299–2301
19. Yao J, Scott JR, Young MK, Wilkins CL (1998) Importance of matrix: analyte ratio for buffer tolerance using 2,5-dihydroxybenzoic acid as a matrix in matrix-assisted laser desorption/ionization-fourier transform mass spectrometry and matrix-assisted laser desorption/ionization-time of flight. J Am Soc Mass Spectrom 9:805–813
20. Chait BT (2006) Chemistry. Mass spectrometry: bottom-up or top-down? Science 314:65–66
21. Cramer R, Gobom J, Nordhoff E (2005) High-throughput proteomics using matrix-assisted laser desorption/ionization mass spectrometry. Expert Rev Proteomics 2:407–420
22. Thiede B, Höhenwarter W, Kraha A, Mattow J, Schmid M, Schmidt F, Jungblut PR (2005) Peptide mass fingerprinting. Methods 35:237–247
23. Bogdanov B, Smith RD (2005) Proteomics by FTICR mass spectrometry: top down and bottom up. Mass Spectrom Rev 24:168–200
24. Zhang G, Annan RS, Carr SA, Neubert TA (2010) Overview of peptide and protein analysis by mass spectrometry. Curr Protoc Protein Sci 16:16.1
25. Henzel WJ, Stults JT (2001) Matrix-assisted laser desorption/ionization time-of-flight mass analysis of peptides. Curr Protoc Protein Sci 16:16.2
26. Lee LT, Wong YK (2010) Pathogenesis and diverse histologic findings of sialolithiasis in minor salivary glands. J Oral Maxillofac Surg 68:465–470
27. Isacsson G, Persson NE (1982) The gigantiform salivary calculus. Int J Oral Surg 11:135–139
28. Epivatianos A, Antoniadis D, Iliadis T, Papanayotou P (1989) Histochemical study on the mucosubstances of the calculi of the main excretory duct of the human submandibular gland. Hell Period Stomat Gnathopathoprosopike Cheir 4:15–20
29. Giray CB, Dogan M, Akalin A, Baltrusaitis J, Chan DC, Skinner HC, Dogan AU (2007) Sialolith characterization by scanning electron microscopy and X-ray photoelectron spectroscopy. Scanning 29:206–210
30. Harrison JD, Epivatianos A, Bhatia SN (1997) Role of microliths in the aetiology of chronic submandibular sialadenitis: a clinicopathological investigation of 154 cases. Histopathology 31:237–251

31. Teymoortash A, Buck P, Jepsen H, Werner JA (2003) Sialolith crystals localized intraglandularly and in the Wharton's duct of the human submandibular gland: an X-ray diffraction analysis. Arch Oral Biol 48:233–236
32. Triantafyllou A, Fletcher D, Scott J (2006) Histological and histochemical observations on salivary microliths in ferret. Arch Oral Biol 51:198–205
33. Jayasree RS, Gupta AK, Vivek V, Nayar VU (2008) Spectroscopic and thermal analysis of a submandibular sialolith of Wharton's duct resected using Nd:YAG laser. Lasers Med Sci 23:125–131
34. Sabot JF, Gustin MP, Delahougue K, Faure F, Machon C, Hartmann DJ (2012) Analytical investigation of salivary calculi, by mid-infrared spectroscopy. Analyst 137:2095–2300, Epub 2012 Mar 14
35. Boskey AL, Burstein LS, Mandel ID (1983) Phospholipids associated with human parotid gland sialoliths. Arch Oral Biol 28:655–657
36. Slomiany BL, Murty VL, Aono M, Slomiany A, Mandel ID (1983) Lipid composition of human parotid salivary gland stones. J Dent Res 62:866–869
37. Ord RA, Pazoki AE (2004) Salivary gland disease and tumors. In: Miloro M (ed) Peterson's principles of oral and maxillofacial surgery, 2nd edn. BC Decker Inc., Hamilton, p 676
38. Koch M, Iro H, Zenk J (2010) Stenosis and other non-sialolithiasis-related obstructions of the major salivary gland ducts. Modern treatment concepts. HNO 58:218–224
39. Schröder JM, Harder J (1999) Human beta-defensin-2. Int J Biochem Cell Biol 31:645–651
40. White SH, Wimley WC, Selsted ME (1995) Structure, function, and membrane integration of defensins. Curr Opin Struct Biol 5:521–527
41. Droin N, Hendra JB, Ducoroy P, Solary E (2009) Human defensins as cancer biomarkers and antitumour molecules. J Proteomics 72:918–927
42. Davison G, Allgrove J, Gleeson M (2009) Salivary antimicrobial peptides (LL-37 and alpha-defensins HNP1-3), antimicrobial and IgA responses to prolonged exercise. Eur J Appl Physiol 106:277–284